

Biomechanical Analysis of the Effect of the Finger Extensor Mechanism on Hand Grasping Performance

Yuyang Wei¹, Zhenmin Zou, Zhihui Qian, Lei Ren², and Guowu Wei³

Abstract—Quantifying the effect of routing and topology of the inter-connected finger extensor mechanism on hand grasping performances is a long-standing research problem for the better clinical diagnosis, surgical planning and biomimetic hand development. However, it is technically demanding to measure the hand performance parameters such as the contact forces and contact area during hand manipulation. It is also difficult to replicate human hand performance through the physical hand model due to its sophisticated musculotendinous structure. In this study, an experimental validated subject-specific finite element (FE) human hand model was used for the first time to quantify the influence of different tendon topologies and material properties on hand grasping quality. It is found that the grasping quality is reduced by 15.94% and 8.54% if there are no extensor hood and lateral band respectively, and the former plays a more important role in transmitting forces and maintaining grasping qualities than the latter. Excluding extensor hood in the topology causes more reductions in hand contact pressure and contact area than omitting lateral band. 7.5% of the grasping quality is lost due to a softened tendon with half of its original Young's Modulus. Hardened extensor tendon does increase the grasping quality, but the enhancing effect tends to level off once the tendon Young's Modulus is increased by more than 50%. These results prove that the lateral band and extensor hood are critical components for maintaining grasping quality. The dexterity and grasping quality of robotic and prosthetic hands could be improved by integrating these two components. There is also no need to use very stiff tendon material as it won't help to effectively enhance the grasping quality.

Index Terms—Extensor mechanism, finite element, human hand model, grasping quality, finger dexterity.

I. INTRODUCTION

DURING daily human activities, the dexterity of fingers and the grasping performance are maintained by the forearm and intrinsic muscles through the musculotendon network

Manuscript received July 6, 2021; revised October 24, 2021 and November 24, 2021; accepted December 12, 2021. Date of publication January 27, 2022; date of current version February 18, 2022. (Corresponding authors: Lei Ren; Guowu Wei.)

Yuyang Wei, Zhenmin Zou, and Lei Ren are with the Department of Mechanical, Aerospace and Civil Engineering, The University of Manchester, Manchester M13 9PL, U.K. (e-mail: lei.ren@manchester.ac.uk).

Zhihui Qian is with the Key Laboratory of Bionic Engineering, Ministry of Education, Jilin University, Changchun 130012, China.

Guowu Wei is with the Institute of Mechanical Engineering, University of Salford, Manchester M5 4WT, U.K. (e-mail: G.Weil@salford.ac.uk).

This article has supplementary downloadable material available at <https://doi.org/10.1109/TNSRE.2022.3146906>, provided by the authors.

Digital Object Identifier 10.1109/TNSRE.2022.3146906

and the constraint forces provided by the joint capsules, ligaments and joint articular surfaces [1], [2]. The dorsal muscle groups located at the human forearm are related with the extension of metacarpophalangeal (MCP) and interphalangeal joints. The extensor digitorum (ED) together with the extensor pollicis longus (EPL) muscle are regarded as the main dorsal forearm muscles for maintaining the grasping capacity. The inter-connected and retinacular ED tendon spanning over the 2nd to 5th digits is recognized as the extensor mechanism or dorsal aponeurosis. This web-like tendon originates from the controlling muscles of the hand and inserts into the phalanges. The muscles associated with hand kinematics are coordinated by a set of retinacular structures of the extensor mechanism to achieve the high dexterity and grasping quality of human hand [3], [4]. The biomechanical functions of these unique features including the lateral band and extensor hood wrapping around the proximal phalangeal joints have attracted attentions from researchers and are regarded as the key structures affecting the hand performance [5]–[7]. The analysis on biomechanics of extensor mechanism and its contributions to grasping capacities may not only help to understand the etiology of hand diseases, surgical planning, but also the design of robotic and prosthetic hand.

Over the past decades, numerous anatomical and biomechanical studies have been carried out to explicitly describe the force transmission mechanism of the human finger musculotendinous system [5], [8]–[11]. However, the muscle force transmission mechanism along this inter-connected extensor network and its effect on human hand grasping performance still remain primitive [3], [4]. The numerical models developed so far were based on conventional equilibrium method without actual tendon topology or adopted the simplified tendon network [9], [10], [12]. The complex temporal and spatial coordination patterns of the multiple musculotendon units were quantified through these numerical and physical muscle-skeleton models. The lateral band of the dorsal aponeurosis was found to be the assister with the interosseous muscles for lateral motion of the MCP joints [4]. It is well known that the material properties and thickness of the extensor mechanism are non-homogenous and the mechanical properties such as the ultimate load, ultimate strain and tangent modulus are significantly varied [5], [13]. However, these heterogeneity of the dorsal aponeurosis were not considered in most of the muscle-skeleton models [5], [14]. As a result, the actual biomechanics and dynamics of the system cannot be

obtained. According to the published studies on biomechanics of extensor mechanism and its effect on grasping performance [5], [9], [11], [12], [15], little is known about the influences of the non-homogenous extensor material and geometry in the musculotendinous force transmission mechanism. There is a strong need to use a realistic numerical human hand model to simulate hand grasping and gain a deeper understanding of the biomechanical effects of the inter-connected extensor mechanism on hand performance.

How the inter-connected hand structure affects the contact forces and dexterity of the fingers is a long-standing research problem which is critical to prosthetic or robotic hand design [3]. Some physical models were developed to closely mimic the anatomy of human hand and study the musculotendinous force transmission and the resulted grasping capabilities [3], [4]. Inouye and Valero-Cuevas [3] improved the grasping quality of a robotic hand through optimizing the phalangeal joint rotation center and routing of extensor lines [3]. Since the biological features and topology of extensor mechanism were not considered in [3], whether these inter-connected soft tissues could enhance the dexterity and grasping quality of robotic and human hand still remains unclear. It is also difficult to use tactile sensors to measure the contact force and contact area. Restoring human hand like performance on physical model is also challenging due to the sophisticated biological musculotendinous system of hand and forearm. So far, little is known about the relationship between the finger extensor mechanism topology and its effects on hand grasping performance while these are critical to the hand surgical planning and the development of the robotic or prosthetic hand [3], [4], [16], [17].

In this research, a validated subject-specific muscle-driven FE human hand model [18] was modified and employed to simulate the realistic soft contact mechanism, and assess the contact force and contact area during hand grasping. The finger extensor mechanism was reconstructed from the MRI data. It was hypothesized that the topological features including extensor hood and lateral band of the extensor mechanism have a significant influence in the grasping quality of human hand. Therefore, the grasping quality of the FE human hand with intact 3D structure of passive extensor mechanism was quantified and compared with the FE hand without the features of lateral band or extensor hood to present their effects on hand performance and contact biomechanics. The grasping quality was measured based on the grasping matrix, contact geometric relations and the limitations of the finger forces for three different grasping.

II. METHODS

A. FE Modelling of the Human Hand and Extensor Mechanism

The muscle-driven FE hand model shown in Fig. 1 was employed to evaluate the grasping performance of hand with different topologies for the extensor mechanism. This FE human hand model can simulate soft contact and predict realistic contact data during hand grasping. It was originally developed in our previous research [18] and was constructed based on the CT and MR images taken from a 24-year-old

male subject, including the intact bone skeleton, subcutaneous tissue and the dermis, epidermis. These anatomical structures were all modelled by solid elements except the ligaments which were simulated using the non-linear spring elements. The material properties of the skin and subcutaneous tissues were defined to be hyper-elastic while linear elastic properties were assigned onto the bone skeleton. *In-vivo* grasping tests were carried out on the same human subject and the electromyography signal of muscles and hand kinematics were captured by using Delsys Trigno (Delsys Inc., Boston, US) and Vicon Systems (Vicon Motion Systems Ltd, Oxford, UK) respectively. The loading and boundary conditions of the FE hand model were defined based on the computed muscle forces and captured hand kinematics. The FE hand model was validated against the *in-vivo* experimental results from three different grasping activities (see Fig.2). More details can be found in [18].

Research has shown that the lateral band and hood structure of the extensor mechanisms are two key components that affect the grasping qualities and finger versatility [4], [19]. Originally, the lateral band and hood structure were modelled by one dimensional wire element in the FE hand model in [18]. This was now modified to restore the biological features of the extensor mechanism in this study. The 3D structures of the extensor mechanism from the distal insertion points at the phalanges to the origin of the extrinsic/intrinsic muscles were generated based on the MR images under the instructions of [20]. The MRI images were taken by using the Ingenia 3.0T (Philips, Best, The Netherlands) with an in-plane resolution of 5μ m, and the slice thickness was 0.3mm. Four extensor mechanisms with different topologies: the intact extensor (IE), the extensor without hood structure (WL), the extensor without lateral band (WH) and the extensor without both hood and band structure (WHL), were modelled (see Fig.2). The whole FE human model consists of 745421 tetrahedral elements (C3D4H) and among them, 144575 elements were used to model the intact extensor mechanism. The extensor mechanisms under different grasping are shown in Fig.3. According to the findings in [16], the material property of the extensor mechanism varies significantly from proximal MCP to distal insertion points, but insignificantly between different fingers. Therefore, the extensor apparatus was divided into seven regions along the central axis from MCP to distal insertion points for the material assignments with different Young's Modulus [21] (see Fig. S1 and Table S1 in the Supplementary Material).

The distal insertion points of the extensor mechanism were bonded to the distal or middle phalanges using 'tie' constraint and the proximal cross-sectional area of the extensor tendon was fixed (see Fig. S2). The 'surface to surface' contact was assigned between the dorsal surface of the bone and the extensor mechanism. Some researchers quantified the friction coefficient between soft tissue and bone or other hard engineering material to study the tribological mechanisms in biological systems [22]–[26]. Most of the measured frictional coefficient ranges from 0.3 to 0.5. Therefore, the average friction coefficient of 0.4 was used in the present FE hand model. The kinematics and muscle forces were assigned

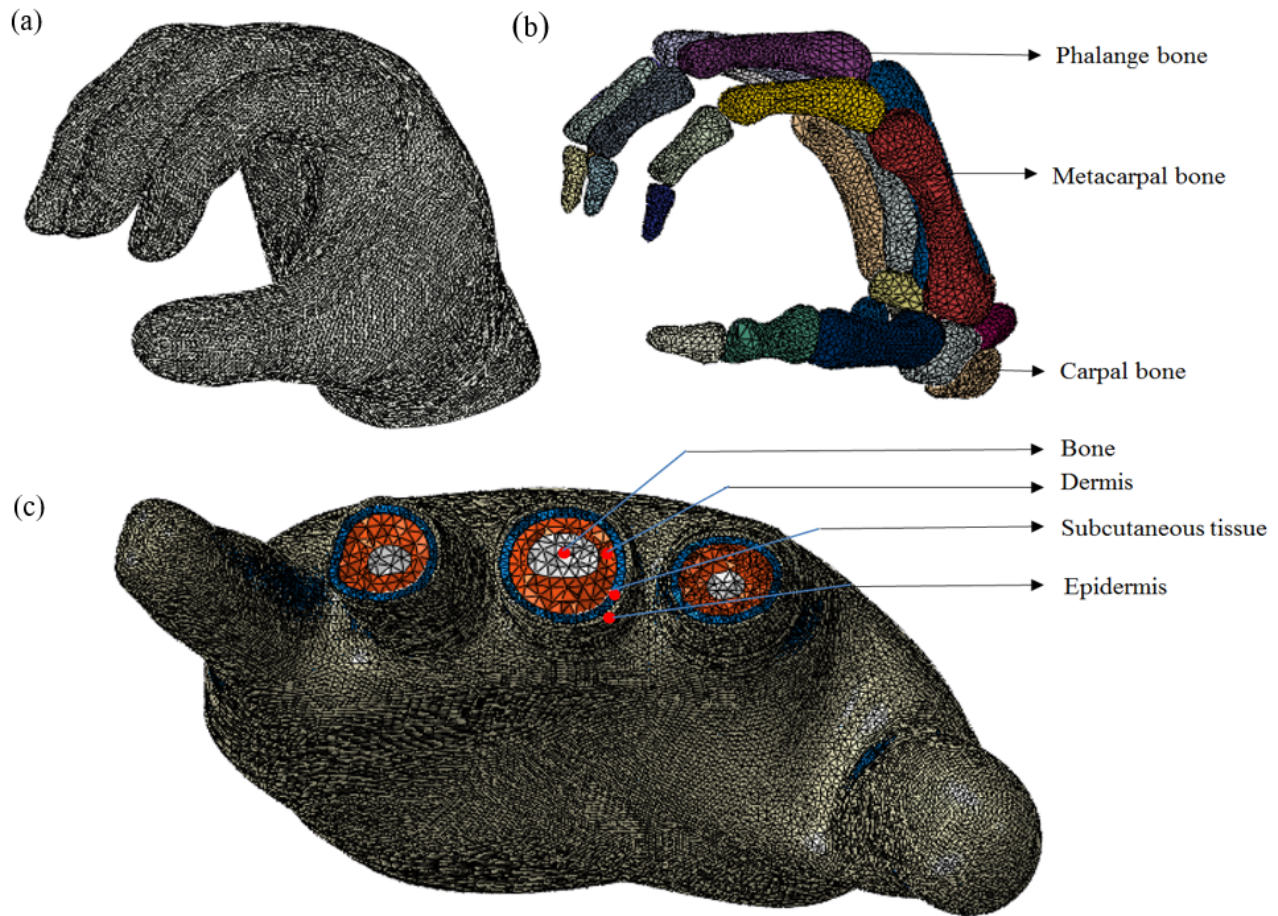


Fig. 1. The FE human hand model. **a.** The subject-specific FE human hand model under grasping posture. The FE hand has 27 degrees of freedom as a real human hand. **b.** The intact bone skeleton of the FE human hand including phalanges, metacarpal and carpal bones. **c.** The four-layered structure of the FE hand including bone skeleton, subcutaneous tissues, dermis and epidermis. The mesh density has been optimized.

based on the experimental measurement from our previous study [18]. Three main extrinsic and six intrinsic muscles associated with hand grasping were selected for measuring the muscle forces according to hand anatomy and the literature [27], [28]. The intrinsic muscle forces including abductor pollicis brevis, dorsal interosseous, flexor pollicis brevis and adductor pollicis were considered during hand grasping (See Fig. S3 and Table S2 in the supplementary material for their positions and magnitudes). The dorsal interosseous muscles forces were applied directly onto the extension hood in this study. The other extrinsic muscle forces were applied onto the corresponding insertion points on the bones of the skeleton. The forearm extensor muscles connecting with the extensor mechanism were not activate during the *in-vivo* grasping experiment. Therefore, the extensor mechanism was regarded as a passive structure and its effect on grasping performance is the primary focus of this study. The muscle forces were estimated based on the electromyography (EMG) signals which were captured by Delsys wireless EMG system (Delsys Inc., Boston, US) during the *in-vivo* grasping test. The subject was asked to sit before a table and the wrist was fixed to perform the isometric grasping. Before the grasping test, maximum voluntary contraction (MVC) tests were carried out for each individual muscle using Jamar dynamometer. The recorded EMG data was band-pass filtered

(20–400 Hz) with a Butterworth filter and then rectified. The muscle forces were then computed based on the maximum voluntary contraction forces. It was assumed that a linear relationship between the EMG signal and muscle force for isometric muscle contracting. A similar method has been used by other researchers to calculate muscle forces under isometric contract [29]–[31].

B. Calculating Hand Grasping Quality

Cylinder, spherical grasping and precision gripping were simulated and assessed to study the effects of the extensor mechanism topology on the human hand grasping qualities. The FE simulation of gripping was conducted in the commercial software ABAQUS (Dassault Systèmes Simulia Corp.). Once the simulation was completed, the contact output parameters such as the contact pressure, contact area, contact normal and shear forces (see Fig. 4) were extracted as the database for the derivation of the grasping quality.

The three components of the contact force, F_x , F_y and F_z , on the contact surface of the grasped object were extracted directly from ABAQUS. So were the three components of the contact moment, M_x , M_y and M_z , about the three coordinate axes on the surface of the grasped object. The external wrench w on the grasped object was then obtained as $\mathbf{w} = [F_x \ F_y \ F_z \ M_x \ M_y \ M_z]^T$ which is in dimension of 6 for

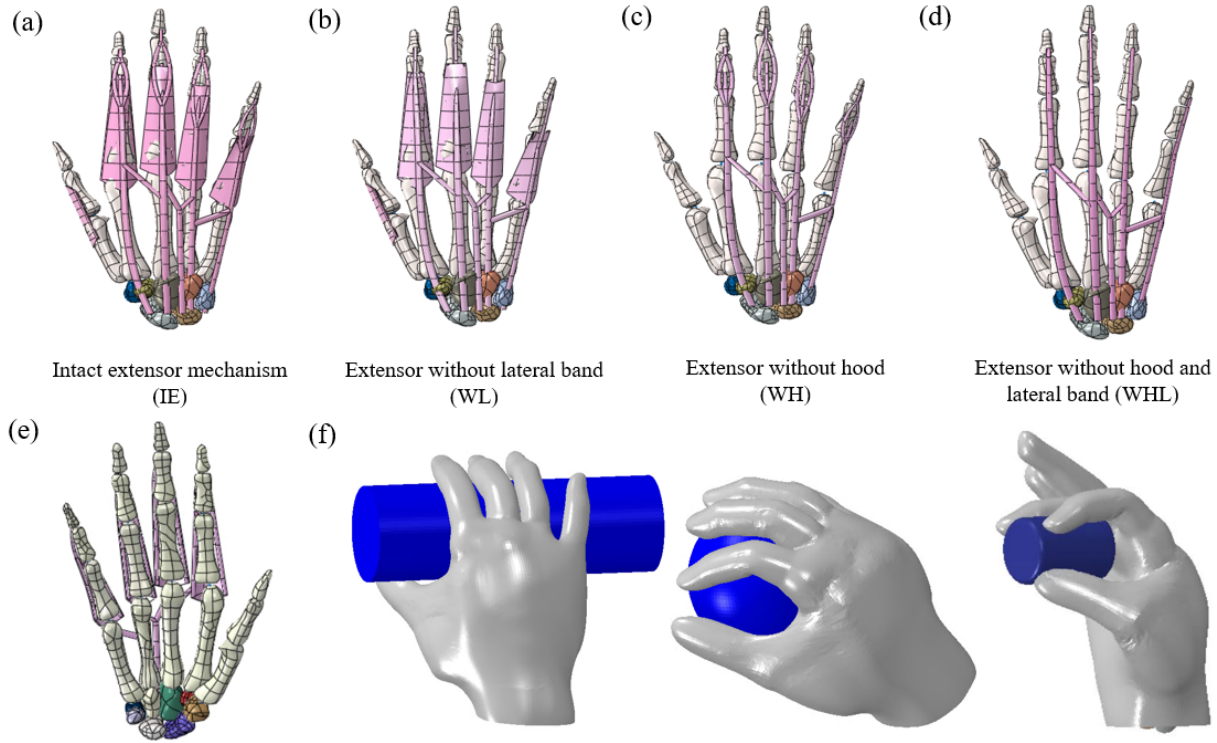


Fig. 2. The four different tendon topologies. (a). The FE human hand baseline model with intact extensor mechanism (IE). (b). The extensor mechanism without hood structure (WH). (c). The extensor mechanism without lateral band (WL). (d). The extensor mechanism without hood structure and lateral band (WHL). (e). The hand skeleton with intact extensor mechanism from palmar view. (f). Simulation of the spherical, cylindrical grasping and precision gripping with FE human hand model.

spatial analysis. Similarly, the three contact force components, f_{xi} , f_{yi} and f_{zi} , on the surface of the i -th finger, and the moment m_{zi} around axis z were extracted directly from ABAQUS. The palm involved in power grasping was regarded as the ‘sixth finger’ in this research. The internal wrench f_c formed by all fingertips and palm involved in the gripping was obtained as $f_c = [f_{x1} f_{y1} f_{z1} m_{z1} \dots f_{xn} f_{yn} f_{zn} m_{zn}]^T$. $n = 3$ for the precision gripping in this research, since three fingers were involved. $n = 6$ for the cylinder and spherical grasping. The internal wrench f_c is related to the external wrench w by the grasping matrix \mathbf{G} as follows [32]:

$$-w = \mathbf{G}f_c \quad (1)$$

Since w and f_c were already obtained from FE simulation, \mathbf{G} was determined from the above equation. Three different groups of criteria were applied to evaluate the grasping quality [32]-[34]. The first one used the measure of the algebraic properties of grasping matrix \mathbf{G} which does not consider forces of the contact points. The second one used the measure based on the geometric relations of grasp which provides the robustness to the grasp. The last grasping quality index is to consider the limitations of the magnitudes of the finger forces. Various grasp quality measures proposed in the literature can be found in the review by Roa and Suárez [32] and the evaluation indices employed in this study are summarized as follows.

1) Measures Based on Algebraic Properties of \mathbf{G} :

a) *Minimum singular value of \mathbf{G}* : The full-rank grasp matrix \mathbf{G} has 6 singular values determined by the positive square roots of eigenvalues of $\mathbf{G}\mathbf{G}^T$. The grasp will lose its capability for

balancing the wrench at least in one direction and the grasp falls into a singular configuration if one of the singular values turns to zero. Therefore, the smallest singular value of \mathbf{G} , $\sigma_{min}(\mathbf{G})$, indicates how far the grasp configurations is from the singular configuration. It is used as one of the grasp quality measure indices [32]:

$$Q_{MSV} = \sigma_{min}(\mathbf{G}) \quad (2)$$

A larger value of $\sigma_{min}(\mathbf{G})$ means a more stable grasp [32].

b) *Volume of the ellipsoid in the wrench space*: The grasp matrix \mathbf{G} can be represented as the mapping from a sphere of unitary radius in the force domain of the contact points into an ellipsoid of the wrench space. The global contribution of all the contact forces can be represented using the volume of this ellipsoid as a quality measure as [32]

$$Q_{VEW} = \sqrt{\det(\mathbf{G}\mathbf{G}^T)} \quad (3)$$

Q_{VEW} should be maximized to obtain the optimum grasp [32].

c) *Grasp isotropy index*: The grasp isotropy index is defined as [32]

$$Q_{GH} = \frac{\sigma_{min}(\mathbf{G})}{\sigma_{max}(\mathbf{G})} \quad (4)$$

$\sigma_{min}(\mathbf{G})$ and $\sigma_{max}(\mathbf{G})$ are the minimum and maximum singular values of \mathbf{G} . When index Q_{GH} is approaching to 1, the grasp turns to be isotropic and uniformly distributed contact forces to the total wrench applied on the object is achieved. Q_{GH} falls to zero when the grasp is close to a singular configuration.

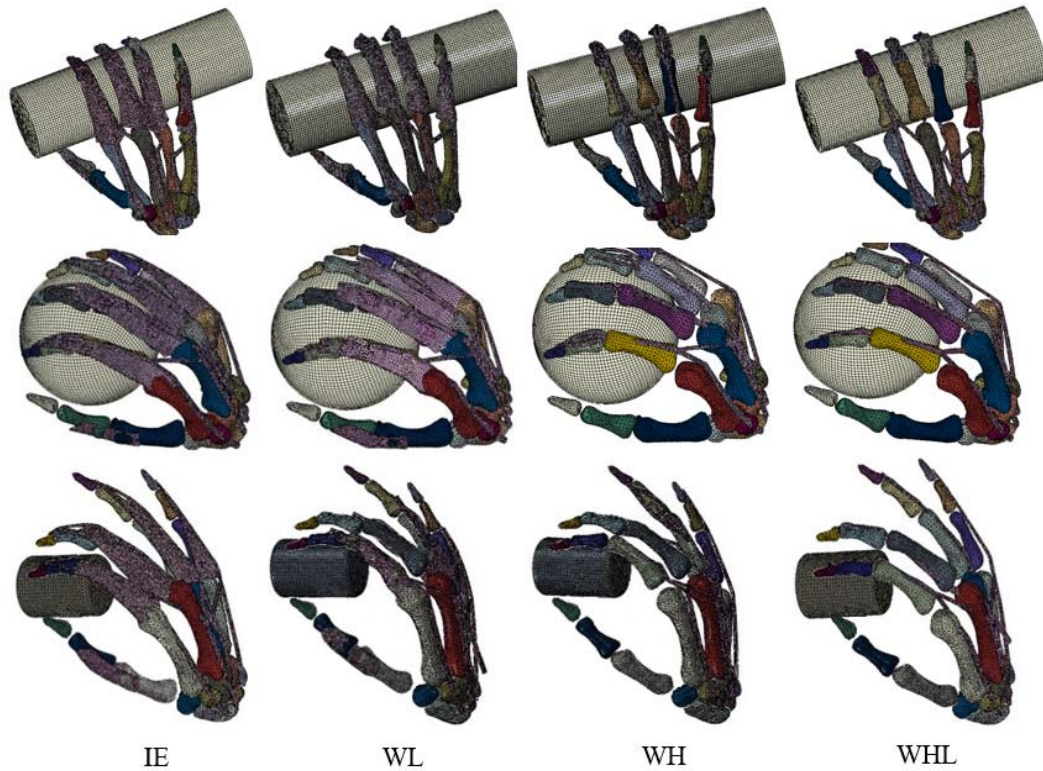


Fig. 3. The extensor tendon with different topologies under cylinder, spherical grasping and precision gripping. The FE human hand model with the intact extensor mechanism (IE), the extensor mechanism without lateral band (WL), the extensor mechanism without hood structure (WH), the extensor mechanism without hood structure and lateral band (WHL) are presented in columns from left to the right. The cylindrical, spherical grasping and precision gripping are shown in rows from top to bottom.

2) Measures Based on Geometric Relations:

a) *Area of the grasp polygon*: For the hard contact of a 3-fingered robotic hand, a larger triangle formed by the contact points on the object produces a more robust grasp since the grasp can resist larger external wrench with bigger contact polyhedron under the same contact forces. Therefore, the area of the grasp triangle is also applied for grasping quality measure. A larger value of this index contributes to a better grasp [32]. In the present study, the grasp polygon was regarded as the hand contact area to meet the soft contact condition of human hand. The actual contact area of the FE human hand was extracted from ABAQUS for this index Q_{GH} .

b) *Distance between the centroid of the contact polygon and the object's center of mass*: The influences of inertial and gravitational forces of grasp are positively proportional to the distance between the object's center of mass and the centroid of contact polyhedron. Therefore, a shorter distance contributes to a better grasp [32]. The distance between the center of the contact area and the center of mass of the grasped object is used for grasping quality measure Q_{DCC} which is extracted from the output of the FE simulation.

3) Measures Based on Limitation of Finger Forces:

a) *Largest-minimum resisted wrench*: The aforementioned two types of quality measures are related with geometric locations of the contact points which do not integrate the finger forces. Considering the force constraints, the magnitude of the perturbation wrench that the grasp can reach under the maximum voluntary contraction forces (MVC) of muscles is

used as one of the grasping quality indices [32].

$$Q_{LRW} = \|\mathbf{w}\| \quad (5)$$

A larger value of Q_{LRW} means a more stable grasp [32].

b) *Normal components of the forces*: The sum of the normal components of the forces applied onto the grasped object represents the force efficiency of the grasp. Therefore, the inverse of the sum of the normal components of the forces is defined as

$$Q_{MNF} = \min \frac{1}{\sum_{i=1}^n f_i^n} \quad (6)$$

The normal contact forces of all the fingers in contact were used to compute the above quality index. Q_{MNF} should be minimized to optimized the grasp [32].

III. RESULTS

The FE hand model with intact extensor mechanism was validated against the *in-vivo* grasping experimental data. The predicted and measured hand contact areas on each finger are shown in Fig.5. There is a good agreement between them. The relative difference between the FE predicted and experiment measured contact area and contact pressure are given in Table I and II. Most of the results are below 10% which is acceptable.

Fig.6 (a) presents the grasping quality changes of the FE human hand with three different extensor tendon topologies compared to the baseline model with the intact extensor tendon

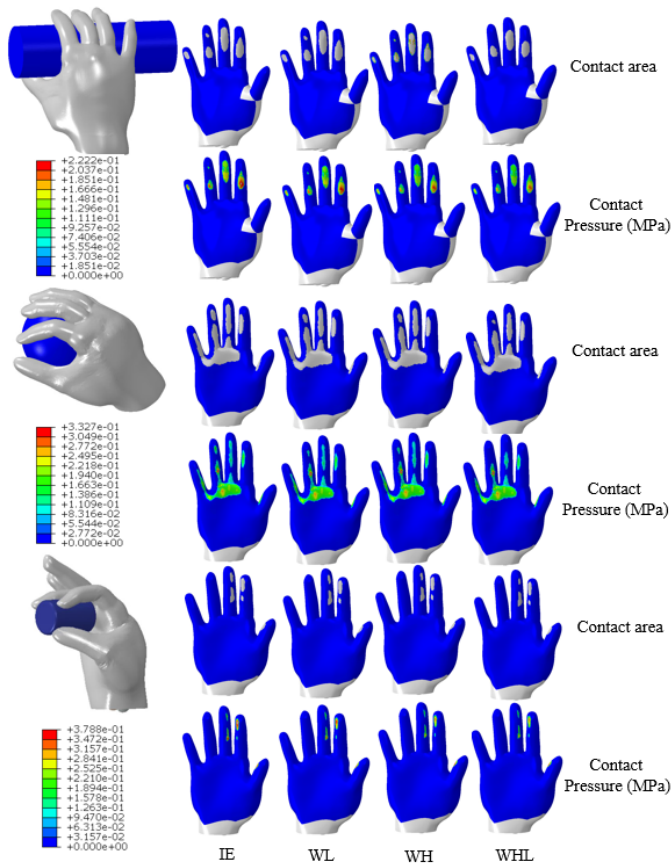


Fig. 4. The contact pressure and contact area output of the three grasping simulations using the FE hand models of four different tendon topologies. The ‘grey zones’ surrounded by blue zone indicate the contact area. The magnitude of contact pressure is illustrated by the scale bar on the left with the unit of MPa.

TABLE I
RELATIVE DIFFERENCE BETWEEN MEASURED AND PREDICTED CONTACT AREA

	Index	Middle	Ring	Little	Thumb
Cylindrical grasping	4.54%	8.23%	7.42%	11.79%	9.58%
Spherical grasping	6.77%	5.79%	5.30%	6.67%	5.05%
Precision gripping	6.88%	5.94%	N/A	N/A	6.71%

TABLE II
RELATIVE DIFFERENCE BETWEEN MEASURED AND PREDICTED CONTACT PRESSURE

	Index	Middle	Ring	Little	Thumb
Cylindrical grasping	9.00%	8.16%	8.58%	11.55%	8.80%
Spherical grasping	8.00%	8.70%	10.42%	9.22%	8.54%
Precision gripping	8.88%	10.21%	N/A	N/A	10.67%

in three grasping postures. These results are the averages of the individual quality measures of the three groups (algebraic properties of grasping matrix, geometric relations, limitations of the finger forces) respectively. The results of the individual quality indices can be found in the supplementary material. As expected, the hand model without hood structure and lateral band (WHL) exhibits the largest loss of grasping

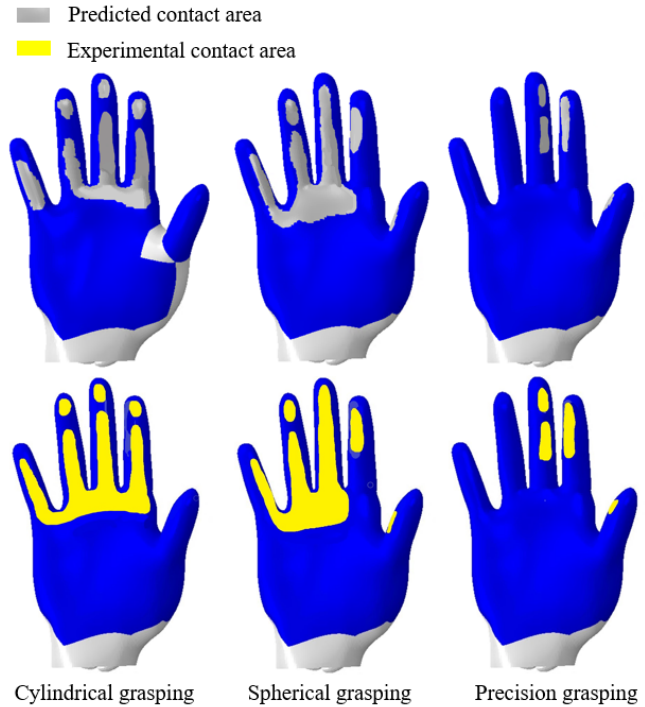


Fig. 5. Comparison of contact area between experimental measurement and FE prediction. The grey zone represents the predicted hand contact area (first row) while the yellow zone represents the measure hand contact area (second row).

qualities among the three different extensor mechanisms for all the three grasping. The grasping quality is reduced by more than 15% in terms of algebraic properties and up to 21.4% for precision gripping. More grasping quality is lost in the precision gripping than in the power grasping when the hand has no hood structure (WH) or has no hood structure and lateral band (WHL). In all cases, the grasping index of algebraic properties of G is more sensitive to the anatomical variations of extensor mechanism than the other two indices are. The effect of Young’s Modulus (E) of the extensor mechanism on the grasping quality is shown in Fig.6 (b). The Young’s Modulus E of the extensor tendon in all regions were adjusted by -50% to +200% of their baseline values. The grasping quality is increased by hardening the extensor mechanisms as indicated by all the quality evaluation indices. The quality increase tends to level off after E is increased by more than +50%. Once again, the index of algebraic properties of G is the most sensitive index to the material variations, gaining approximately 20% increase in precision gripping while the other indices achieve about more than 10% increment, except the geometric relations in spherical grasping with 7.1% increase.

The simulation results of the grasping activities suggest that the variations of grasping quality could be initiated by the contact parameters including contact area or contact forces. The variations of contact forces, contact pressure and contact area are displayed in Fig.7 for different tendon topologies, the magnitudes were extracted and integrated over the whole hand contact area during different grasping. Most of the contact parameters are decreased by more than 20% by excluding the

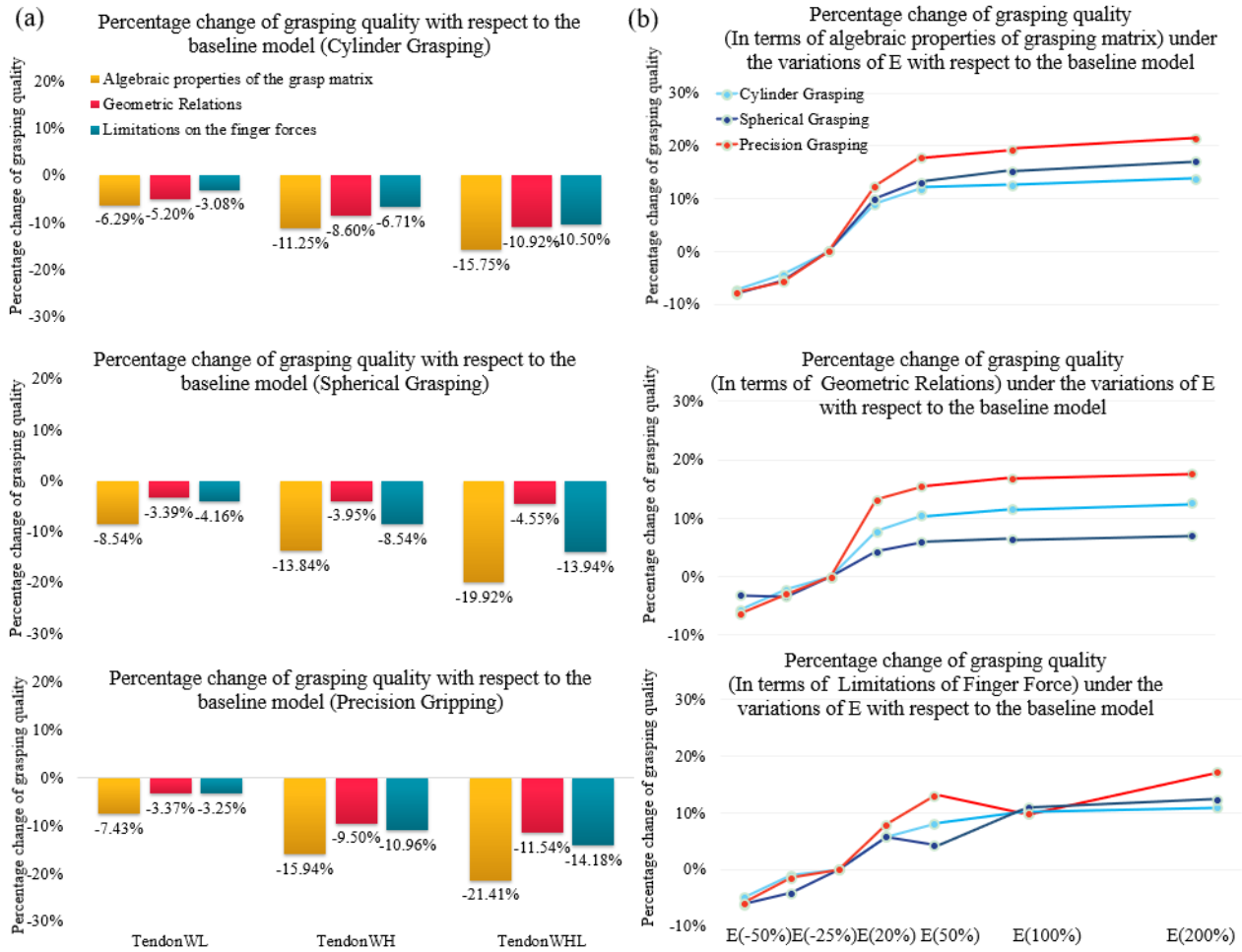


Fig. 6. The effects of simplified tendon topologies and material properties on the grasping qualities of the FE human hand under cylinder, spherical grasping and precision gripping. (a). The FE hand models with the extensor mechanism of IE, WL, WH, WHL were studied. The grasping qualities were compared with their counterpart from the base line model (IE) with intact extensor tendon and the difference was shown in percentage. Three grasping quality indices: algebraic properties of grasping matrix, geometric relations and finger force limitations were quantified separately. (b). The grasping qualities of the FE human hand with different Young's Modulus for extensor mechanisms. The Young's Modulus of the extensor tendon was adjusted from -50% to $+200\%$ and the resulted variations on grasping quality were derived and compared with the baseline model.

lateral band and the extensor hood in the hand model. Most of the contact parameters are reduced by more than 15% when the hand loses its extensor hood. Losing lateral band causes only less than 10% reduction in the contact parameters.

IV. DISCUSSION

The extensor mechanism of human hand is an anatomically sophisticated inter-connected and retinacular structure with non-homogeneous, viscoelastic material properties [20], [21], [35]. Understanding the mechanical behavior of finger extensor mechanism and its effects on grasping and dexterity are critical to hand surgical planning, robotic and prosthetic hand development [1], [16], [17], [36], [37]. The anatomical topology and mechanical properties of the extensor tendon has been studied for a long time [4]–[6], [10], [38]. Although it was found that they are critical components, their effects on grasping quality and finger dexterity have not been quantified properly using the physical hand models. This is due to the difficulties on restoring the musculotendinous system, soft contact of human hand through the physical model and the demanding measurements on contact forces and area [3].

To overcome these difficulties, we employed a validated muscle-driven subject-specific FE human hand model to simulate hand grasp activities in this study. Hence, all the contact parameters are estimated reasonably well and subsequently the grasping qualities under different tendon topologies are reliably assessed.

The grasping qualities of human hand during power grasping and precision gripping were correlated with the retinacular structures of extensor mechanism. The lateral band and extensor hood both help to transmit forces and maintain grasping qualities. If extensor hood is missing in the extensor mechanism, the normal and shear contact forces at the fingertips will be reduced by 16.35% and 17.22% respectively as shown in Fig. 7. Missing lateral band reduces the contact force and area by 9.50% and 9.96% respectively. The lateral band plays less important role than extensor hood in the extensor mechanism. This is consistent with the finding in the hand model with intact extensor mechanism that the lateral band experiences less tension than the extensor hood. Due to the decrease of the finger contact forces and contact area (See Fig.7), the wrench space becomes distorted, and this affects the algebraic

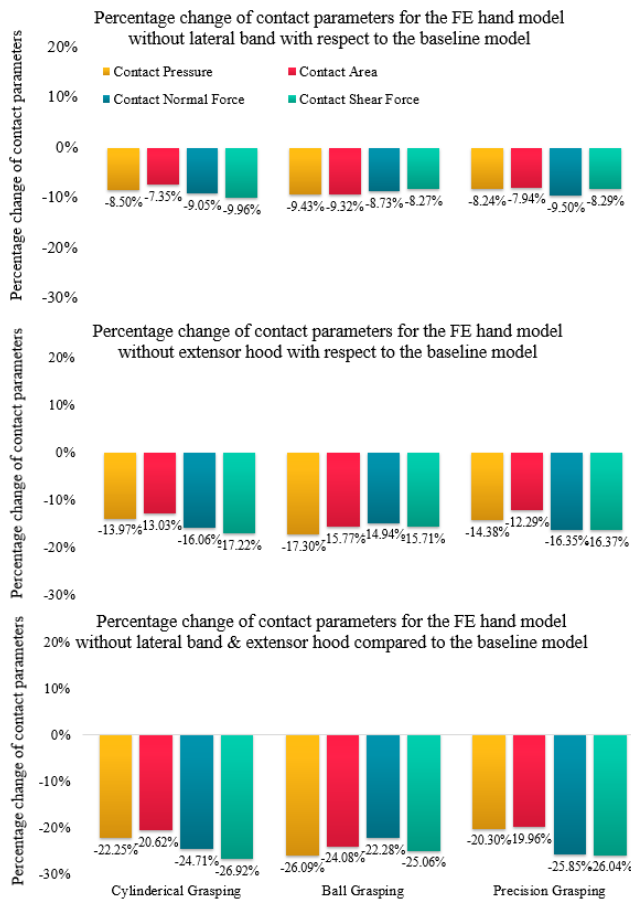


Fig. 7. The effect of tendon topologies on the contact pressure, contact area and contact forces on the FE human hand. The normal and shear contact forces were extracted over the whole contact area. The FE hand models with the extensor mechanism of IE, WH, WL, WHL were studied under cylinder, spherical grasping and precision gripping. The contact results or parameters were compared with the base line model (IE) with intact extensor tendon.

properties of grasp matrix. The results in Fig.6 (a) show that missing lateral band and extensor hood can reduce the grasping quality by as high as 8.54% and 15.94%, respectively. Once again, the lateral band shows less effect than the extensor hood. The shrinking of the contact area due to the lack of the retinacular tissues causes the drifting of the centroid of the contact polygon and then affects the geometric-relations-based grasping quality index. However, very little reduction (less than 5%) in this type of quality measures is found during spherical grasping. This may be due to the fact that the position of the centroid of contact polygon is only affected very slightly by the shrinking of the contact area, so is the distance between the mass centre of the object and centroid of contact polygon.

The finger-force-limitations based grasping quality index is significantly affected by the absence of the extensor hood and lateral band as shown in Fig.6 (a). The reason is obvious that the extensor hood and lateral band connect with the lumbrical and interossei muscles which are critical for coordinating musculoskeletal system to generate appropriate finger forces [19], [39]. Among the three groups of grasping quality measures, the algebraic properties of G tend to be the most sensitive index to the modifications of extensor topology. It may be more effective to use the algebraic properties to

quantify grasping quality. Larger reductions in the grasping quality index are observed in precision gripping than in the power grasping. Improving and achieving human hand like dexterity and precision control capacity on robotic and prosthetic hand is a persistent problem to researchers [40]–[43]. The presented results prove that integrating the extensor mechanism into the robotic and prosthetic hand may help to improve the dexterity and grasping quality since these retinacular tissues connected with intrinsic muscles help to provide constraints, maintain normal kinematics and transmit musculotendon forces to the fingers.

The material property and thickness of the finger extensor mechanism are non-homogeneous according to the anatomical studies. Some *in-vitro* experiments have been conducted to measure the material properties of the extensor mechanism [13], [21]. The effect of this non-homogenous material assignment was quantified and analyzed through our FE human hand model in this research. The Young's Modulus in different regions of the extensor mechanism were changed from -50% to $+200\%$ from their baseline values and the resulted grasping qualities were evaluated. If the tendon is softened by halving its Young's Modulus, 7.5% of the hand grasping quality will be lost. Increasing Young's Modulus by 50% enhances the grasping quality by 15.5%. The hardened extensor tendon may produce a larger mechanical impedance of the fingers and the contact forces, leading to better algebraic properties of the grasp matrix and larger shape of contact polygon. However, the quality improvement does not continue all the time as the tendon gets hardened and hardened. It tends to level off after the Young's Modulus of the tendon is increased by more than 50% of its original value, achieving a 21.63% improvement. Therefore, there is no need to use very stiff material in the artificial extensor mechanism of the biomimetic or prosthetic hand as it might not be able to enhance the hand performance effectively.

As for the limitations of this study, first, the biomechanics of hand grasping is sophisticated, there are other factors such as the finger joint rotation axis [3] and the friction between extensor tendon [4] and bone skeleton that can also affect the hand grasping performance. Moreover, the extensor mechanism was regarded as a passive structure during the three grasping simulations. Further investigations are required to consider a wider range of hand manipulating or postures with an activated extensor mechanism. Finally, viscoelastic or anisotropic material properties could be used for extensor tendon to achieve more accurate tensile behavior.

V. CONCLUSION

To the best of our knowledge, we are the first to employ a muscle-driven FE human hand model to investigate hand grasping performance and quantify the effect of the interconnected retinacular tissues on finger versatility and manipulation capability. This study has confirmed that the lateral band and extensor hood are the key components of the extensor mechanism contributing to the grasping quality. It is found that soft structures that are similar to the extensor hood and lateral band in the human hand should be integrated into the robotic or prosthetic hand to enhance its dexterity and grasping capacity. Whereas there is no need to use very stiff tendon material for

the extensor mechanism as it does not help effectively enhance the grasping quality. The algebraic property of grasping matrix might be the most effective index for evaluating grasp quality. The muscle-driven FE human model can predict detailed and reliable contact parameters during hand grasping. Combined with the grasping performance evaluating criteria, this model can be employed to provide quantified view into the biomechanical functions of the different components of the hand. It is a trustworthy numerical model that provides inspirations for developing robotic and prosthetic hand.

ACKNOWLEDGMENT

The authors acknowledge The University of Manchester for providing computing resources. They would also like to thank Dr. Zhuo Wang from The First Bethune Hospital of Jilin University for his help with the MRI and CT scan. The authors declare that they have no conflicts of interest.

REFERENCES

- [1] S. T. Tan and P. J. Smith, "Anomalous extensor muscles of the hand: A review," *J. Hand Surg.*, vol. 24, no. 3, pp. 449–455, May 1999.
- [2] R. L. Lieber, M. D. Jacobson, B. M. Fazeli, R. A. Abrams, and M. J. Botte, "Architecture of selected muscles of the arm and forearm: Anatomy and implications for tendon transfer," *J. Hand Surg.*, vol. 17, no. 5, pp. 787–798, Sep. 1992.
- [3] J. M. Inouye and F. J. Valero-Cuevas, "Anthropomorphic tendon-driven robotic hands can exceed human grasping capabilities following optimization," *Int. J. Robot. Res.*, vol. 33, no. 5, pp. 694–705, Apr. 2014.
- [4] D. D. Wilkinson, M. V. Weghe, and Y. Matsuoka, "An extensor mechanism for an anatomical robotic hand," in *Proc. IEEE Int. Conf. Robot. Autom.*, Sep. 2003, pp. 238–243.
- [5] D. Hu, L. Ren, D. Howard, and C. Zong, "Biomechanical analysis of force distribution in human finger extensor mechanisms," *BioMed Res. Int.*, vol. 2014, pp. 1–9, Jul. 2014.
- [6] N. Ogihara, "An anatomically based 3-D musculo-skeletal model of the human hand for evaluation of precision grip capabilities," *Amer. J. Phys. Anthropol. Suppl.*, vol. 40, pp. 159–160, 2005.
- [7] F. J. Valero-Cuevas, V. V. Anand, A. Saxena, and H. Lipson, "Beyond parameter estimation: Extending biomechanical modeling by the explicit exploration of model topology," *IEEE Trans. Biomed. Eng.*, vol. 54, no. 11, pp. 1951–1964, Nov. 2007.
- [8] B. Weightman and A. A. Amis, "Finger joint force predictions related to design of joint replacements," *J. Biomed. Eng.*, vol. 4, no. 3, pp. 197–205, Jul. 1982.
- [9] J. N. A. L. Leijnse, "Why the lumbrical muscle should not be bigger—A force model of the lumbrical in the unloaded human finger," *J. Biomech.*, vol. 30, nos. 11–12, pp. 1107–1114, Nov. 1997.
- [10] Z. M. Li, V. M. Zatsiorsky, and M. L. Latash, "Contribution of the extrinsic and intrinsic hand muscles to the moments in finger joints," *Clin. Biomechanics*, vol. 15, no. 3, pp. 203–211, Mar. 2000.
- [11] C. T. Jadelis, "Index finger extensor hood mechanics using finite element and rigid body dynamic modeling," Tech. Rep., 2020.
- [12] K. N. An, E. Y. Chao, W. P. Cooney, and R. L. Linscheid, "Normative model of human hand for biomechanical analysis," *J. Biomech.*, vol. 12, no. 10, pp. 775–788, Jan. 1979.
- [13] J. F. Weber, A. M. R. Agur, A. Y. Fattah, K. D. Gordon, and M. L. Oliver, "Tensile mechanical properties of human forearm tendons," *J. Hand Surg. Eur. Volume*, vol. 40, no. 7, pp. 711–719, Sep. 2015.
- [14] D. Hu, D. Howard, and L. Ren, "Biomechanical analysis of the human finger extensor mechanism during isometric pressing," *PLoS ONE*, vol. 9, no. 4, Apr. 2014, Art. no. e94533.
- [15] Z.-M. Li, V. M. Zatsiorsky, and M. L. Latash, "The effect of finger extensor mechanism on the flexor force during isometric tasks," *J. BioMech.*, vol. 34, no. 8, pp. 1097–1102, 2001.
- [16] Y. Hirai, K. Yoshida, K. Yamanaka, A. Inoue, K.-I. Yamaki, and M. Yoshizuka, "An anatomic study of the extensor tendons of the human hand," *J. Hand Surg.*, vol. 26, no. 6, pp. 1009–1015, Nov. 2001.
- [17] R. McMurtry and J. Jochims, "Congenital deficiency of the extrinsic extensor mechanism of the hand," *Clin. Orthopaedics Rel. Res.*, vol. 125, pp. 36–39, Jun. 1977.
- [18] Y. Wei, Z. Zou, G. Wei, L. Ren, and Z. Qian, "Subject-specific finite element modelling of the human hand complex: Muscle-driven simulations and experimental validation," *Ann. Biomed. Eng.*, vol. 48, no. 4, pp. 1181–1195, 2019.
- [19] B. A. Cloud, J. W. Youdas, N. J. Hellyer, and D. A. Krause, "A functional model of the digital extensor mechanism: Demonstrating biomechanics with hair bands," *Anatomical Sci. Educ.*, vol. 3, no. 3, pp. 144–147, 2010.
- [20] J. A. Clavero, P. Golanó, O. Fariñas, X. Alomar, J. M. Monill, and M. Esplugas, "Extensor mechanism of the fingers: MR imaging-anatomic correlation," *Radiographics*, vol. 23, no. 3, pp. 593–611, May 2003.
- [21] K. Qian, K. Traylor, S. W. Lee, B. Ellis, J. Weiss, and D. Kamper, "Mechanical properties vary for different regions of the finger extensor apparatus," *J. Biomechanics*, vol. 47, no. 12, pp. 3094–3099, Sep. 2014.
- [22] S. Shacham, D. Castel, and A. Gefen, "Measurements of the static friction coefficient between bone and muscle tissues," Tech. Rep., 2010.
- [23] Z. Jin and D. Dowson, "Bio-friction," *Friction*, vol. 1, no. 2, pp. 100–113, Jun. 2013.
- [24] H. Forster and J. Fisher, "The influence of loading time and lubricant on the friction of articular cartilage," *Proc. Inst. Mech. Eng., H, J. Eng. Med.*, vol. 210, no. 2, pp. 109–119, Jun. 1996.
- [25] J. F. Ramírez and J. A. Vélez, "Incidence of the boundary condition between bone and soft tissue in a finite element model of a trans-femoral amputee," *Prosthetics Orthotics Int.*, vol. 36, no. 4, pp. 405–414, 2012.
- [26] J. Parekh, D. E. Shepherd, D. W. Hukins, C. Hingley, and N. Maffulli, "In vitro investigation of friction at the interface between bone and a surgical instrument," *Proc. Inst. Mech. Eng., H, J. Eng. Med.*, vol. 227, no. 6, pp. 712–718, Jun. 2013.
- [27] F. H. Netter, *Atlas of Human Anatomy E-Book*. Amsterdam, The Netherlands: Elsevier Health Sciences, 2017.
- [28] C. L. Taylor and R. J. Schwarz, "The anatomy and mechanics of the human hand," *Artif. limbs*, vol. 2, no. 2, pp. 22–35, May 1955.
- [29] F. D. Farfán, J. C. Politti, and C. J. Felice, "Evaluation of EMG processing techniques using information theory," *Biomed. Eng. OnLine*, vol. 9, no. 1, p. 72, Dec. 2010, doi: 10.1186/1475-925X-9-72.
- [30] C. J. De Luca, L. D. Gilmore, M. Kuznetsov, and S. H. Roy, "Filtering the surface EMG signal: Movement artifact and baseline noise contamination," *J. Biomech.*, vol. 43, no. 8, pp. 1573–1579, May 2010, doi: 10.1016/j.jbiomech.2010.01.027.
- [31] T. J. Butler, S. L. Kilbreath, R. B. Gorman, and S. C. Gandevia, "Selective recruitment of single motor units in human flexor digitorum superficialis muscle during flexion of individual fingers," *J. Physiol.*, vol. 567, no. 1, pp. 301–309, Aug. 2005.
- [32] M. A. Roa and R. Suárez, "Grasp quality measures: Review and performance," *Auto. Robots*, vol. 38, no. 1, pp. 65–88, 2015.
- [33] A. Bicchi and V. Kumar, "Robotic grasping and contact: A review," in *Proc. ICRA. Millennium Conf. IEEE Int. Conf. Robot. Automat. Symposia*, Apr. 2000, pp. 348–353.
- [34] T. Singh and S. Ambike, "A soft-contact and wrench based approach to study grasp planning and execution," *J. Biomech.*, vol. 48, no. 14, pp. 3961–3967, Nov. 2015.
- [35] J. A. Clavero *et al.*, "MR imaging of ligament and tendon injuries of the fingers," *RadioGraphics*, vol. 22, no. 2, pp. 237–256, Mar. 2002.
- [36] T. P. Schweitzer and G. M. Rayan, "The terminal tendon of the digital extensor mechanism: Part II, kinematic study," *J. Hand Surg.*, vol. 29, no. 5, pp. 903–908, Sep. 2004.
- [37] M. A. Wehbé, "Anatomy of the extensor mechanism of the hand and wrist," *Hand Clinics*, vol. 11, no. 3, pp. 361–366, Aug. 1995.
- [38] H. Lipson, "A relaxation method for simulating the kinematics of compound nonlinear mechanisms," Tech. Rep., 2006.
- [39] B. Wang *et al.*, "Engineering of extensor tendon complex by an ex vivo approach," *Biomaterials*, vol. 29, no. 20, pp. 2954–2961, Jul. 2008.
- [40] J. Zhou *et al.*, "A soft-robotic approach to anthropomorphic robotic hand dexterity," *IEEE Access*, vol. 7, pp. 101483–101495, 2019.
- [41] J. T. Belter and A. M. Dollar, "Performance characteristics of anthropomorphic prosthetic hands," in *Proc. IEEE Int. Conf. Rehabil. Robot.*, Jun. 2011, pp. 1–7.
- [42] W. Chen, C. Xiong, and S. Yue, "Mechanical implementation of kinematic synergy for continual grasping generation of anthropomorphic hand," *IEEE/ASME Trans. Mechatronics*, vol. 20, no. 3, pp. 1249–1263, Jun. 2015.
- [43] L. U. Odhner *et al.*, "A compliant, underactuated hand for robust manipulation," *Int. J. Robot. Res.*, vol. 33, no. 5, pp. 736–752, Apr. 2014.